Numerical analysis of the performance of a resonant gravity-wave detector

Bu-Xin Xu, W. O. Hamilton, W. W. Johnson, N. D. Solomonson, and O. D. Aguiar
Department of Physics and Astronomy, Louisiana State University, Baton Rouge, Louisiana 70803-4001
(Received 3 March 1989)

This paper presents the results of a detailed numerical calculation of the performance of a resonant gravitational radiation detector which uses an inductive transducer and a superconducting quantum interference device amplifier. We demonstrate the correctness of the calculations by comparing them to the present performance of the Louisiana State University antenna. We show that a standard cryogenic resonant bar detector operating at 4 K is capable of a noise temperature of less than 0.75 mK, corresponding to an rms gravitational-wave amplitude of 1.9×10^{-19}.

I. INTRODUCTION

The second-generation gravitational-wave detectors which use cryogenic techniques and superconducting instrumentation are now beginning to report results.[1–3] Most recently, for example, from March to October of 1988 the detector at Louisiana State University[4] (LSU) operated with a gravitational-wave[5] noise amplitude $h=2.2\times10^{-18}$. A coincidence search with this new generation of detectors has been carried out and many more results should be expected within the next few years.[6]

Although about 5 orders of magnitude in detection energy sensitivity have been achieved over Weber's original room-temperature detector, the low-temperature detectors are still in the initial stage of operation. In this paper we make a detailed numerical analysis of the performance of our cryogenic gravitational-wave detector. This is not only helps us to understand the present detector operation, but also gives us insight for further improvements. We will see that by extending existing measurement technology and by operating at millikelvin temperatures, another 3–5 orders of magnitude improvement in detection energy sensitivity may be achieved.

Our description of the performance of a resonant gravitational-wave detector is based on a calculation of the noise spectral density at the output of the detector. The detector noise expression determines the detector noise temperature, and the detector noise temperature together with the antenna cross section determines the detection sensitivity. The cryogenic gravitational wave detector at LSU consists of a 5056 aluminum Weber-type antenna, a Paik-type transducer,[7] and a superconducting quantum interference device (SQUID) amplifier. Our configuration is very similar to that of the gravitational-wave detector at Stanford University.[8,9] Several authors have previously estimated the sensitivity of such detectors.[10–12] Michelson and Taber made a first detailed calculation of signal-to-noise ratio for the detector at Stanford by modeling the SQUID as a conventional linear current amplifier.[13,14]

The dc SQUID is the most sensitive magnetic field sensor so far available and is particularly suitable for a gravitational-wave detector which uses a modulated inductive transducer. Tesche[15] and others have pointed out that an analysis using conventional linear amplifier circuits does not adequately model the behavior of a dc SQUID amplifier. They demonstrate that the behavior of a dc SQUID in a circuit cannot simply be described by the SQUID's isolated parameters. Therefore we present here a different analysis with a view to explicitly exploring the interaction between the gravity-wave antenna, transducer, and dc SQUID. We use this analysis to relate the detector noise temperature to the SQUID's intrinsic parameters and to achieve an optimal coupling between

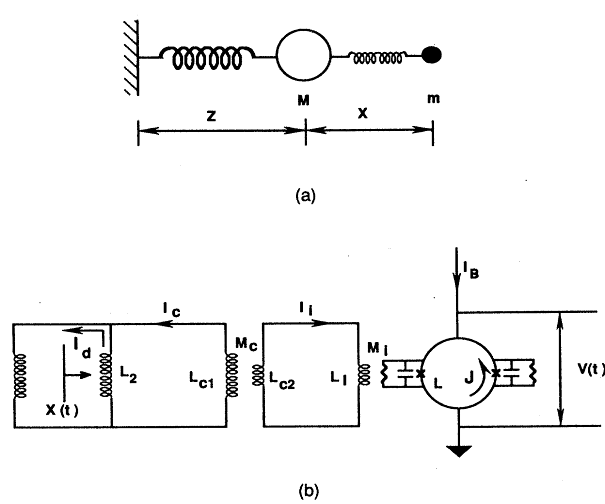

FIG. 1. Schematic of a resonant gravity-wave detector with a modulated inductance transducer and a dc SQUID. (a) Gravitational-wave antenna and transducer diaphragm as two coupled harmonic oscillators. (b) Coupling of transducer and dc SQUID. Two flat coils of superconducting wire L_1 and L_2 are rigidly mounted on the antenna and are set to face opposite sides of the diaphragm. These two coils are connected to the superconducting transformer which is chosen to achieve impedance matching between the transducer and the SQUID input.

antenna, transducer, and amplifier. We begin with a complete set of motion equations for the gravity-wave antenna, transducer, and dc SQUID (Refs. 16 and 17). Although the motion equation for the dc SQUID is nonlinear we are still able to get an analytic form of noise expression by using Tesche and Clarke's numerical analysis results for the dc SQUID (Refs. 18 and 19).

We demonstrate the equations of motion in the Appendix. The result for the noise spectral density of the resonant gravitational-wave antenna modeled by Fig. 1 is

$$S_n(\omega)=S_V^0(\omega)+\frac{V_\phi^2|m^{-1}c^2W_2(\omega)-b|^2}{|1+bJ_\phi-m^{-1}c^2J_\phi W_2(\omega)|^2}S_J^0(\omega)+2\,\mathrm{Re}\left[\frac{V_\phi[m^{-1}c^2W_2(\omega)-b]}{1+bJ_\phi-m^{-1}c^2J_\phi W_2(\omega)}\right]S_{VJ}^0(\omega)$$
$$+\frac{c^2V_\phi^2m^{-2}|W_2(\omega)|^2}{|1+bJ_\phi-m^{-1}c^2J_\phi W_2(\omega)|^2}S_f(\omega)+\frac{c^2V_\phi^2m^{-2}|W_1(\omega)|^2}{|1+bJ_\phi-m^{-1}c^2J_\phi W_2(\omega)|^2}S_F(\omega)\,, \tag{1}$$

where $W_1(\omega)$ and $W_2(\omega)$ are response functions:

$$W_1(\omega)=\frac{(m/M)\omega^2}{G_1(\omega)G_2(\omega)-\omega^2(m/M)\left[\omega_t^2+j\frac{\omega_t\omega}{Q_t}\right]}\,, \tag{2}$$

$$W_2(\omega)=\frac{G_1(\omega)-(m/M)\omega^2}{G_1(\omega)G_2(\omega)-\omega^2(m/M)\left[\omega_t^2+j\frac{\omega_t\omega}{Q_t}\right]}\,, \tag{3}$$

$$G_1(\omega)=\left[\omega_a^2-\omega^2+j\frac{\omega_a\omega}{Q_a}\right]\,, \tag{4}$$

$$G_2(\omega)=\left[\omega_t^2-\omega^2+j\frac{\omega_t\omega}{Q_t}\right]\,; \tag{5}$$

$$b=\frac{M_i^2(L_{c1}+L_0/2)}{(L_{c1}+L_0/2)(L_{c2}+L_i)-M_c^2}$$

is the SQUID low-frequency effective inductance ;

$$c=\frac{M_iM_cI_d\alpha}{(L_{c1}+L_0/2)(L_{c2}+L_i)-M_c^2}$$

is the displacement-flux transfer function ;

$$V_\phi=\partial\bar{V}/\partial\phi$$

is the flux-voltage transfer function ;

$$J_\phi=\partial\bar{J}/\partial\phi$$

is the flux-current transfer function; $S_V^0(\omega)$, $S_J^0(\omega)$, and $S_{VJ}^0(\omega)$ are SQUID voltage noise, circulating current noise, and voltage-current correlation noise spectral densities, respectively; $S_f(\omega)$ and $S_F(\omega)$ are the Nyquist force spectral densities associated with the dissipation in the transducer and the antenna, respectively; and m and M, Q_t and Q_a, ω_t and ω_a denote the effective mass, quality factor, and angular resonant frequency for the uncoupled transducer and antenna, respectively.

The signal response at the SQUID output to an impulse depositing energy ϵ in the antenna is

$$|V_s(\omega)|^2=2M\epsilon|A(\omega)|^2$$
$$=2M\epsilon\left|\frac{cV_\phi m^{-1}W_1(\omega)}{1+bJ_\phi-m^{-1}c^2J_\phi W_2(\omega)}\right|^2\,. \tag{6}$$

The detector noise temperature can then be determined. According to the theory of matched filters the noise temperature is[9,20,21]

$$T_n=\frac{\pi}{k_BM}\left[\int_{-\infty}^{\infty}\frac{|A(\omega)|^2}{S_n(\omega)}d\omega\right]^{-1}\,. \tag{7}$$

The mathematical form of all of these expressions is rather complicated. Therefore their implications and the dependence of the noise temperature on various system parameters can be best displayed in numerical form. In the next section we show the results of our numerical calculations.

II. RESULTS AND CONCLUSIONS

The first goal of our numerical analysis was to understand the sensitivity of the present LSU detector. The LSU antenna is currently operating with a transducer which has a very light diaphragm and which is read out by a BTI rf SQUID. We show the system parameters of the 1988 LSU experiment in Table I. Using these parameters and Eq. (1) we calculate the noise contributions from the individual terms in Eq. (1). The results are shown in Fig. 2. The SQUID voltage-current correlation noise term has been neglected in this example since the value S_{VJ}^0 for the rf SQUID has not been measured but is estimated to be small. In Fig. 3 we compare the calculat-

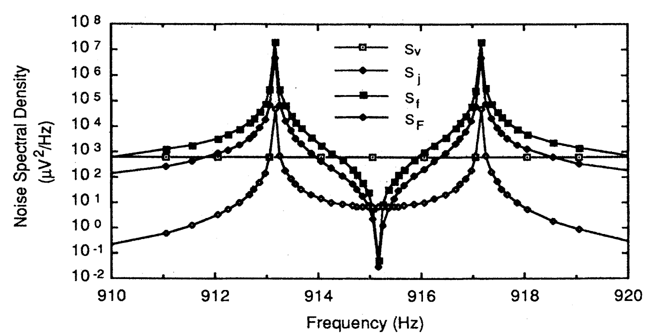

FIG. 2. Noise contributions at the SQUID output from the individual terms in Eq. (1) calculated for the parameters of the 1988 LSU detector run.

TABLE I. 1988 LSU system parameters.

Antenna mass	2296 kg
Antenna frequency	915.149 Hz
Antenna quality factor	9.7×10^{6}
Transducer diaphragm effective mass	0.0221 kg
dc current in transducer at resonance	4.2 A
Mode frequencies	
Plus mode	917.0896 Hz
Minus mode	913.0768 Hz
Mode quality factors	
Plus mode	4.09×10^{4}
Minus mode	3.93×10^{4}
SQUID white noise density at output	7.56×10^{-10} V^2/Hz
SQUID flux-voltage transfer function	9.67×10^{13} V/Wb

ed total noise density with experimental results. The solid line shows a summation of the individual noise contributions in Fig. 2 and the points show the results directly recorded from a HP 3561A signal analyzer. In Fig. 4 we show the calculated signal-to-noise ratio (SNR) density for a 1-K energy impulse on the antenna. Integrating the area under this curve gives the detector noise temperature which, in this case, is 105 mK. We have analyzed our recorded experimental data using numerical matched filters.[22] The experimental noise temperature varies between 96 mK and 115 mK depending on the day. We have also measured the SNR density by driving the antenna with white noise through a separate calibrator. The result is displayed by the points in Fig. 4.

Inspired by the fairly good agreement between the numerical calculation and the experimental results, we carried our numerical calculation further and investigated the quantitative dependence of the detector noise temperature on various transducer and SQUID parameters. The LSU group has operated several dc SQUID's fabricated in Clarke's group at Berkeley. The best energy sensitivity of these particular SQUID's is $369\hbar$. The parameters of these SQUID's have been very carefully measured.[17] The optimum parameter β ($=2LI_0/\Phi_0$) is very close to 1 and therefore the current noise and correlation noise are well defined.[18] In the following calculations we assumed SQUID parameters as shown in Table II. The parameters such as SQUID voltage noise density and flux-voltage transfer functions are based on our measurements of the Clarke dc SQUID's (Ref. 17). The parameters such as current noise density in the SQUID loop and the current-voltage correlation noise density are extrapolated from the Clarke-Tesche dc SQUID theory.[18,19] For all of the calculations reported here the denominator of all terms in Eq. (1) has been set equal to 1. This step is justified by the design of all the transducers used to date. We are concerned, in particular, with the influence of the SQUID parameters on the optimum transducer parameters.[23] Figure 5 shows the dependence of the detector noise temperature on the transducer resonator mass as a function of antenna-transducer quality factor and SQUID noise parameters. For a given antenna mass, the optimum value of transducer mass depends only weakly on the antenna-transducer quality factor and SQUID parameters. However, a light transducer mass severely degrades detector performance. Our present transducer has an effective mass $m=0.022$ kg which is far from optimum. Our correctly designed transducer has an effective mass $m=0.3$ kg, which should continue to be optimum within a wide range of antenna-transducer quality factor and dc SQUID parameters.

In Fig. 6 we show the dependence of the detector noise

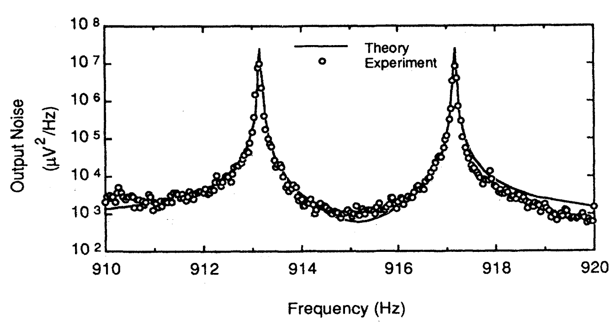

FIG. 3. Total noise at the SQUID output in the 1988 LSU detector run. Points are experimental data, and the solid line is calculated from Eq. (1).

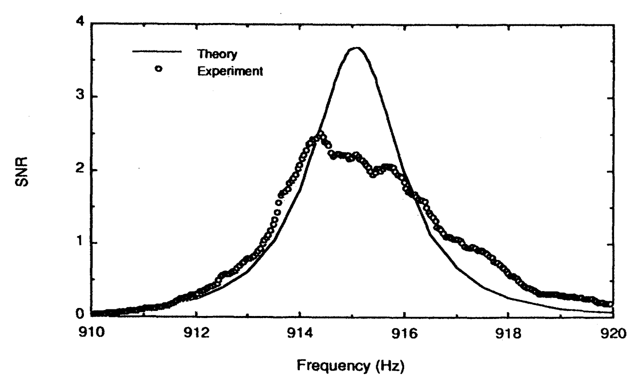

FIG. 4. Distribution of signal-to-noise ratio in 1988 LSU detector run. The solid line is calculated from Eqs. (1) and (6), and the points are experimental data.

TABLE II. SQUID parameters used in calculations.

SQUID type	$S_V^0(\mu V^2/Hz)$	$S_J^0(\mu A^2/Hz)$	$S_{VJ}^0(\mu V \mu A/Hz)$	V_ϕ (V/Wb)	Figure
Clarke 1000 $\hbar$	13.5×10^{-9}	2.5×10^{-10}	16.8×10^{-10}	1.26×10^{10}	5(a)
Clarke 300 $\hbar$	5.56×10^{-9}	1.06×10^{-10}	6.95×10^{-10}	1.5×10^{10}	5,6,7,8,9
$3\hbar$ (50 mK)	6.62×10^{-11}	1.26×10^{-12}	8.28×10^{-12}	1.5×10^{10}	10
Tesche and Clarke	$16k_BTR$	$11k_BT/R$	$12k_BT$	R/L	

temperature on the antenna-transducer quality factor when an optimum transducer mass and a $300\hbar$ dc SQUID is used. It is well known that detector noise temperature will continually improve with the increase of antenna-transducer quality factor. However, its numerical form is not quite clear. The results in Fig. 6 tell us that for a detector using a SQUID amplifier with an energy sensitivity of $300\hbar$, the improvement of the noise temperature is gradual after the transducer and antenna reach a high-Q value. Further improvement in noise temperature can only be achieved by improving SQUID performance. This feature of the relative requirement of the SQUID performance and antenna-transducer Q factor is more clearly shown in Fig. 7. In Fig. 7 we display the dependence of detector noise temperature on SQUID voltage noise at various antenna and transducer levels. In this calculation, we also assume SQUID current noise density and voltage-current correlation noise density change proportionally with S_V^0. Physically this corresponds to cooling the SQUID.

It is interesting to study the noise contribution from the SQUID amplifier. Figure 8 shows the SQUID noise contribution when different noise sources are considered. The contribution of SQUID current noise includes two parts. The first part arises from the back action of the SQUID noise current on the transducer circuit. This part is relatively small since $b=0.13\times10^{-9}$ H in the LSU detector. The second part arises from the back ac-

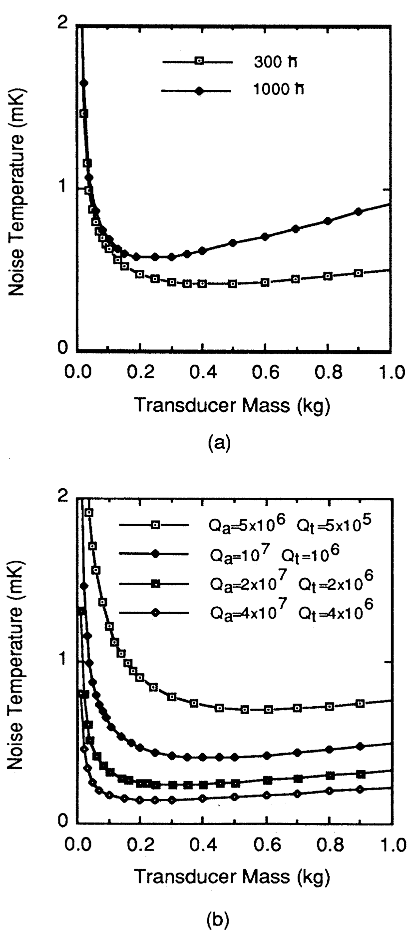

FIG. 5. Noise temperature of a resonant gravity-wave detector vs transducer mass as a function of (a) SQUID energy sensitivity and (b) antenna-transducer quality factor with a $300\hbar$ SQUID.

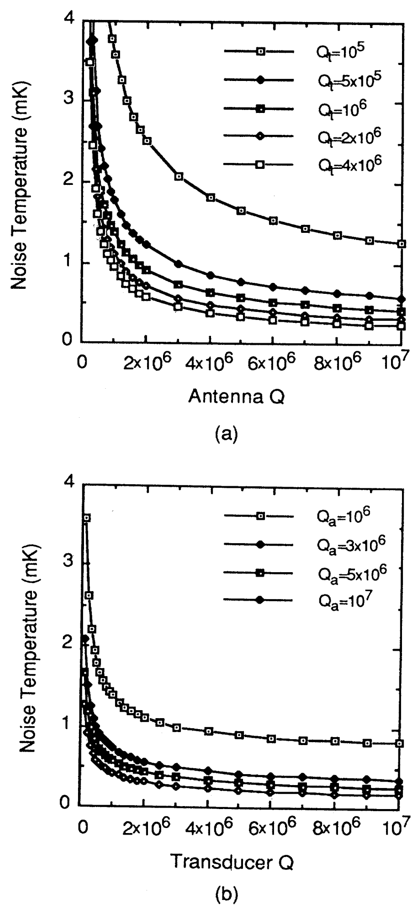

FIG. 6. (a) Noise temperature of a resonant gravity-wave detector vs Q_a as a function of Q_t. (b) Noise temperature of a resonant gravity-wave detector vs Q_t as a function of Q_a.

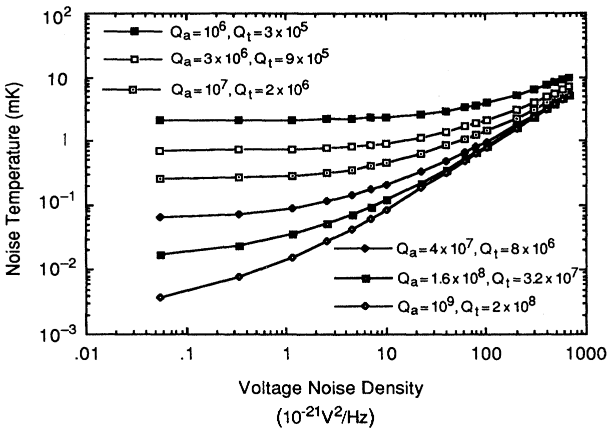

FIG. 7. Noise temperature of a resonant gravity-wave detector vs SQUID voltage noise as a function of antenna-transducer quality factors.

tion of the SQUID noise current on the antenna-transducer mechanical oscillator. An important feature of Fig. 8 is that the correlation contribution changes sign at the two resonant peaks. Therefore the correlation contribution will not significantly influence the detector noise temperature but it does change the SNR density when SQUID noise is dominant.

In Fig. 9 we examine the possibility of improving the noise temperature by reducing SQUID inductance and junction capacitance. Clarke and Tesche concluded that the optimum performance of a dc SQUID is obtained when $\beta \equiv 2LI_0/\Phi_0 = 1$ and $\beta_c \equiv 2\pi I_0 R^2 C/\Phi_0 \approx 1$. This results in optimum energy resolution[21]

$$E/(1\ \text{Hz}) = 16 k_B T (LC)^{1/2} ,$$

where L is the inductance of the SQUID loop, C is the capacitance of the junction, and R and I_0 are the shunt resistance and critical current of each junction, respectively. Here we directly compute the dependence of gravitational-wave detector noise temperature on SQUID inductance as a function of antenna-transducer Q factor. In this calculation we suppose that mutual inductance between the SQUID input coil and the SQUID loop $M_i^2 = \gamma^2 L_i L$ changes with L, but that γ and L_i remain

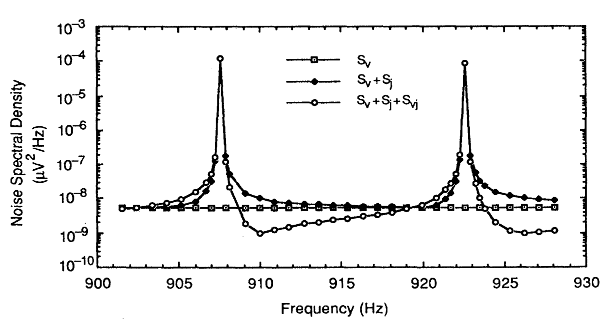

FIG. 8. SQUID noise contribution when different noise sources are considered.

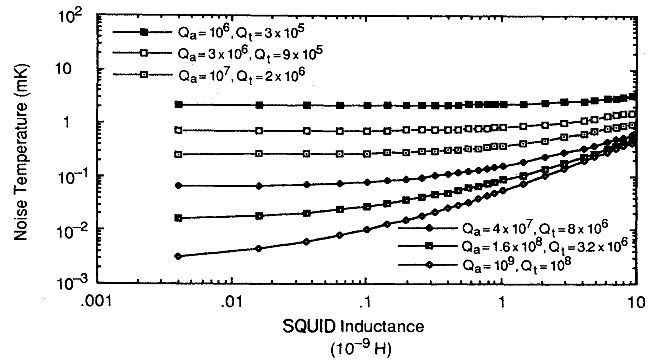

FIG. 9. Noise temperature of a gravity-wave detector vs SQUID inductance as a function of antenna-transducer quality factors.

constant. We also assume that the SQUID shunt resistance is fixed, and that the SQUID noise spectral densities keep the values shown in Table II. The SQUID V_ϕ increases as the SQUID loop inductance L decreases and therefore the SQUID energy sensitivity is improved. The results in Fig. 9 show that the detector noise temperature

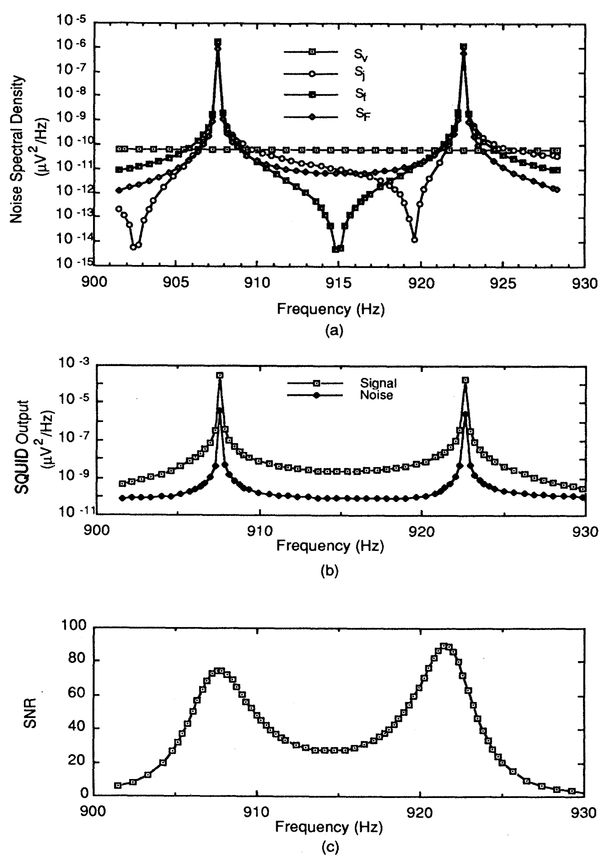

FIG. 10. Prospective performance of the LSU gravity-wave detector at 50-mK operating temperature. (a) Noise contributions at the SQUID output from the sources of Eq. (1). (b) Total noise and the response to a gravity-wave signal at SQUID output. (c) SNR distribution and resulting noise temperature. The integral of the curve gives a detector noise temperature of 0.94 μK.

continually improves as L is reduced, especially when both the antenna and transducer possess extremely high Q factors.

In a final exercise we illustrate the prospective performance of a gravitational-wave antenna such as the LSU gravitational-wave detector when the detector is operated at a temperature of 50 mK and is equipped with a $3\hbar$ dc SQUID (Refs. 24 and 25). Figure 10 shows the total system noise, the response of the detector to a 1-mK impulse on the antenna, and the resulting SNR density. Integrating the area under the SNR curve gives a detector noise temperature 0.94 μK, which is 5 orders of magnitude lower than the present LSU detector noise temperature. A similar calculation to that shown in Fig. 6 indicates that an antenna quality factor $Q_a = 8\times 10^7$ and a transducer quality factor $Q_t = 1.5\times 10^7$ would be required to get this low detector noise temperature. Preliminary results[26] do indicate that the mechanical losses in aluminum 5056 continue to decrease as the temperature is reduced so this performance may be realizable.

In summary, we have compared our numerical analysis with experimental data from the present operating gravitational-wave detector and achieved reasonable agreement. The dependence of detector noise temperature on various system parameters has been carefully calculated. With these numbers we anticipate a noise temperature of about 5 mK in the next run of the gravitational-wave detector at LSU. This improvement will be achieved by using our inductively coupled "mushroom" transducer which has an effective mass of approximately 0.3 kg and which will be amplified by a commercial BTI dc SQUID. Use of a Clarke or similar dc SQUID would achieve a noise temperature of less than 1 mK. After that, another 3 orders of magnitude improvement in noise temperature is still possible by the use of dilution refrigeration technology and the use of a $3\hbar$ dc SQUID operating at 50 mK.

ACKNOWLEDGMENTS

This research was supported in part by LSU and by the National Science Foundation under Grant No. PHY 87-00441.

APPENDIX

The equations of motion are derived from the circuit shown in Fig. 1. We treat the two junctions in the dc SQUID as identical with the same capacitance and shunt resistance. We use the conservation of magnetic flux in each superconducting loop of the SQUID and transducer as well as the mechanical equations of motion to obtain the equations

$$m\ddot{X} + H_2\dot{X} + K_2X = -\alpha I_d I_c + f - m\ddot{Z} \ ,$$

$$M\ddot{Z} + H_1\dot{Z} + K_1 Z = \alpha I_d I_c - f + K_2X + H_2\dot{X} + F + F_s \ ,$$

$$I_c = \frac{M_c M_i \bar{J} + (L_{c2} + L_i)\alpha I_d X(t)}{(L_{c1} + L_0/2)(L_{c2} + L_i) - M_c^2} \ ,$$

$$I = -\frac{M_i (L_{c1} + L_0/2)\bar{J} + M_c \alpha I_d X(t)}{(L_{c1} + L_0/2)(L_{c2} + L_i) - M_c^2} \ ,$$

$$\left[\frac{\Phi_0}{2\pi}\right]^2 \frac{\beta_c}{RI_0}\frac{d^2\delta_1}{dt^2} + \frac{\Phi_0}{2\pi}\frac{d\delta_1}{dt} = \frac{RI_b}{2} - RJ - RI_0\sin\delta_1 + V_{N1} \ ,$$

$$\left[\frac{\Phi_0}{2\pi}\right]^2 \frac{\beta_c}{RI_0}\frac{d^2\delta_2}{dt^2} + \frac{\Phi_0}{2\pi}\frac{d\delta_2}{dt} = \frac{RI_b}{2} + RJ - RI_0\sin\delta_2 + V_{N2} \ ,$$

$$\left[\frac{\Phi_0}{2\pi}\right](\delta_1 - \delta_2) = LJ + b\bar{J} - cX + \Phi_b \ .$$

The definition of b and c is given in the text above. α is the modulation parameter, i.e., $L_1 = L_0 + \alpha X(t)$ and $L_2 = L_0 - \alpha X(t)$. δ is the phase shift across the junction. I_d is the current circulating in the transducer loop. J is the instantaneous current circulating in the SQUID loop while $\bar{J}$ is the time-averaged circulating current. It should be noted that the current coupled to the input coil from the SQUID will not be the instantaneous SQUID current at the Josephson frequency because the circuit impedances will not allow it. Combining the above equations and defining the following terms we may arrive at the noise power spectral density S_n given above as Eq. (1):

$$\omega_a^2 = \frac{K_1}{M} \ ,$$

$$\omega_t^2 = \left[\frac{1}{m}\right]\left[K_2 + \frac{(L_{c1} + L_i)\alpha^2 I_d^2}{(L_{c1} + L_0/2)(L_{c2} + L_i) - M_c^2}\right] \ ,$$

$$Q_t = \frac{\omega_t m}{H_2}, \quad Q_a = \frac{\omega_a M}{H_1} \ .$$

[1]P. F. Michelson, M. Bassan, C. Bowdery, W. M. Fairbank, M. S. McAshan, B. Moskowitz, J. Price, T. Stevenson, and R. C. Taber, paper presented at GR-11, Stockholm, July, 1986. See, also, *Proceedings of the 11th International Conference on General Relativity and Gravitation,* Stockholm, Sweden, 1986, edited by M. A. H. MacCallum (Cambridge University Press, Cambridge, England, 1987), p. 313.

[2]G. Pizzella, E. Amaldi, P. Bonifazi, P. Carelli, M. G. Castellano, G. Cavallari, E. Coccia, C. Cosmelli, and V. Foglietti, paper presented at GR-11, Stockholm, July, 1986. See, also, *Proceedings of the 11th International Conference on General Relativity and Gravitation* (Ref. 1), p. 313.

[3]W. O. Hamilton, Bu-Xin Xu, A. G. Mann, G. Wang, N. Solomonson, and A. Sibley, paper presented at GR-11, Stockholm, July, 1986. See also *Proceedings of the 11th International Conference on General Relativity and Gravitation* (Ref. 1), p. 313.

[4]W. O. Hamilton, Bu-Xin Xu, W. W. Johnson, N. Solomonson, O. D. Aguiar, B. Price, J. Harper, G. Griffin, and D. Duncan, in *Proceedings of Fifth Marcel Grossmann Meeting on General*

Relativity, Perth, Australia, 1988, edited by D. Blair and M. J. Buckingham (World Scientific, Singapore, 1989).

[5]The noise temperature and rms conventional gravitational-wave amplitude for a cylindrical antenna of mass M and length L are related by the equation

$$h=(\pi/8)(2/L)(4k_B T_N/M\omega^2)^{1/2} .$$

[6]E. Amaldi *et al.*, Astron. Astrophys. **216**. 325 (1989).

[7]H. J. Paik, Ph.D. dissertation, Stanford University, 1974.

[8]P. F. Michelson, J. C. Price, and R. C. Taber, Science **227**, 109 (1987).

[9]W. M. Fairbank, M. Bassan, E. R. Mapoles, M. S. McAshan, P. F. Michelson, and B. E. Moskowitz, in *Proceedings of the Fourth Marcel Grossmann Meeting on General Relativity,* Rome, Italy, 1985, edited by R. Ruffini (North-Holland, Amsterdam, 1986).

[10]H. J. Paik, Nuovo Cimento **55B**, 15 (1980).

[11]R. P. Giffard, Phys. Rev. D **14**, 2478 (1976).

[12]J.-P. Richard, J. Appl. Phys. **60**, 3807 (1986).

[13]P. F. Michelson and R. C. Taber, J. Appl. Phys. **52**, 4313 (1981).

[14]P. F. Michelson and R. C. Taber, Phys. Rev. D **29**, 2149 (1984).

[15]C. D. Tesche, Appl. Phys. Lett. **41**, 490 (1982).

[16]Bu-Xin Xu and W. O. Hamilton, J. Appl. Phys. **57**, 1729 (1985).

[17]Bu-Xin Xu, Ph.D. dissertation, Louisiana State University, 1985.

[18]C. D. Tesche and J. Clarke, J. Low Temp. Phys. **29**, 301 (1977).

[19]C. D. Tesche and J. Clarke, J. Low Temp. Phys. **37**, 397 (1979).

[20]W. W. Johnson, Bu-Xin Xu, B. Price, and W. O. Hamilton, paper presented at the International Workshop on GW Signal Analysis and Processing, Amalfi, Italy, 1988 (unpublished).

[21]E. Amaldi, C. Cosmelli, G. V. Pallottino, G. Pizzella, P. Rapagnani, and F. Ricci, Nuovo Cimento **9C**, 829 (1986).

[22]E. Amaldi, G. Pizzella, P. Rapagnani, and F. Ricci, Nuovo Cimento **9C**, 51 (1986).

[23]W. O. Hamilton, W. W. Johnson, Bu-Xin Xu, N. Solomonson, O. D. Aguiar, A. G. Mann, A. Sibley, and B. Price, in the *Proceedings of International Symposium on Experimental Gravitational Physics,* edited by P. F. Michelson, Hu Enke, and G. Pizzella (World Scientific, Singapore, 1987), p. 388.

[24]D. D. Awschalom, J. Warnock, J. M. Hong, L. L. Chang, M. B. Ketchen, and W. J. Gallagher, Phys. Rev. Lett. **62**, 199 (1989).

[25]D. D. Awschalom *et al.*, Appl. Phys. Lett. **53**, 2108 (1988).

[26]William Duffy, University of Santa Clara, private communication.